Microcapsules Prepared via Pickering Emulsion Polymerization for Multifunctional Coatings

Bei Qian[a, b], Zhaoliang Zheng[b], Chengbao Liu[c], Man Li[d], Raechelle A. D'Sa[d], Haiyan Li[b], Michael Graham[b], Marios Michailidis[b], Pavel Kantserev[e], Vladimir Vinokurov[e], Dmitry Shchukin[b, e*]

[a] *College of Chemistry and Pharmaceutical Sciences, Qingdao Agricultural University, 700 Changcheng Road, Qingdao 266109, PR China.*

[b] *Stephenson Institute for Renewable Energy, Department of Chemistry, University of Liverpool, Crown Street, Liverpool L69 7ZD, U.K.*

[c] *Ningbo Institute of Materials Technology and Engineering, Chinese Academy of Science, Ningbo 315201, China.*

[d] *Department of Mechanical, Materials and Aerospace Engineering, University of Liverpool, Liverpool L69 3GH, U.K.*

[e] *Gubkin University, 19991, 65/1 Leninsky prospect, Moscow, Russia.*

Keywords: Pickering emulsion; self-healing; antimicrobial; localized electrochemical impedance spectroscopy

Abstract: Micro/nanocontainer-based self-healing coatings have achieved enormous interest in scientific community during the last decade. However, the search for multifunctional micro/nanocontainers still has research challenge, especially for the micro/nanocontainers with dual functionality (both anticorrosion and antimicrobial). Here, a novel type of microcapsules with antimicrobial shell and anticorrosion core was prepared by the Pickering emulsion polymerization technique. Dimethyloctadecyl [3-(trimethoxysilyl) propyl] ammonium chloride (QC18) and linseed oil were encapsulated as the antimicrobial and the anticorrosion agents, respectively. The results of local electrochemical impedance spectroscopy (LEIS) at 10 Hz demonstrated corrosion suppression in the scratched area of coatings doped with multifunctional microcapsules. Additionally, the QC18-modified microcapsules exhibited high antibacterial performance, showing over 90 % antimicrobial efficacy against gram-positive bacteria. This type of dual-functional coating might guide future design of micro/nanocontainer-based self-healing paint formulations.

1. Introduction

The cost of marine corrosion is increasing every year. The National Association of Corrosion Engineers (NACE)'s IMPACT study has estimated that the total cost of marine corrosion worldwide is between $50 and $80 billion every year. In addition to this intrinsic properties of seawater (e.g., chloride content, efficient electrolyte, and splash zones), microorganism-induced corrosion (MIC) also causes the deterioration of

metallic structures. A large part of the economic losses in the marine industry is caused by MIC [1-5].

Isolating the corroding metal from the seawater through intact coating is one of the main methods for controlling the corrosion of metals in seawater. However, the coating's barrier effects against corrosion are jeopardized due to mechanical vulnerability during transportation or service [6]. The self-healing coatings that possess rapid feedback activity in response to these attacks is a prospective solution [7,8]. After some pioneering works by the authors of this study [9-14], research related to self-healing coatings has gained tremendous attention in the recent decades [15-17]. Majority of these previous works had only focused on the anticorrosion property of the coatings. As previously mentioned, MIC should not be ignored when marine corrosion is discussed. Thus, endowing self-healing coatings with anticorrosion and antibacterial properties is interesting.

Different encapsulation methods have been used to fabricate micro/nanocapsules filled with inhibitors or active agents [18,19]; such methods can endow the coatings with intelligent self-healing properties. Polymerization is a well-established method for the fabrication of micro/nanocapsules [8]. Pickering emulsions are stabilized by solid colloidal particles, which act as emulsifiers at the oil/water interface [20]. The type of emulsion can be determined by the three-phase angle θ_{ow}. Oil-in-water (o/w) emulsions prefer hydrophilic particles ($\theta_{ow} < 90^{o}$), whereas stable inversion emulsions (w/o) are usually obtained by hydrophobic particles ($\theta_{ow} > 90^{o}$) [21,22]. Compared with the

particle's thermal energy, extremely higher energy is needed to remove it from the interface. Pickering emulsions are fantastic precursors to the formation of micro/nanocapsules from the environmental aspects. Moreover, the surface of the Pickering reservoirs can be modified by functional molecules because their shell has the properties of pure nanoparticles [23]. This feature fulfils the aforementioned requirements for multifunctional coatings.

The present study focuses on a new type of micro/nanocapsules based on Pickering emulsions with dual self-healing and antibacterial functions. In our previous works, Pickering nanocontainers in a water-based anticorrosive coating were introduced [23,24]. Polysulfone (PSF)/SiO_2 hybrid capsules were prepared using linseed oil as a core material for self-healing anticorrosion effect and surface-modified Ludox TMA particles as a stabilizer. This easy-to-operate microencapsulation method was developed to prepare the self-lubricating composites in the previous work [25]. The quaternary ammonium salts were used to make the surface of silica particles active as antibacterial agents, which can be adsorbed on the negatively charged bacterial cell membranes, leading to cell death [26].

2. Experimental section

2.1. Materials

Ludox TMA suspension (silica, 34 wt % suspension in H_2O, particle size of 22 nm, surface area 180 m^2/g), linseed oil (0.93 g/mL), PSF (1.24 g/mL) and dichloromethane

(DCM) (≥ 99.8%, 1.325 g/mL) were purchased from Sigma-Aldrich UK. Dimethyloctadecyl [3-(trimethoxysilyl) propyl] ammonium chloride (QC18, 60% in methanol) was purchased from Acros Organics. Bisphenol diglycidyl either ($C_{21}H_{24}O_4$, 1.17 g/mL) and trithylenetetramine ($C_6H_{18}N_4$, 0.98 g/mL) curing agent were purchased from Alfa Aesar. The carbon steel electrodes with an area of 1 cm^2 were polished by 400 and 800 sand papers and cleaned in acetone and ethanol using ultrasonic treatment. Staphylococcus aureus (ATCC 29213 strain), LB broth and LB agar broth were purchased from Sigma. Deionized water was used throughout the study.

2.2. Preparation of microcapsules

Three methods were used to prepare modified Pickering microcapsules encapsulated with linseed oil. Silica was modified by QC18 before emulsification (Method 1), after emulsification (Method 2), and after polymerization (Method 3). The details of Methods 1 and 2 are described in the Supporting Information. Either Method 1 or 2 failed due to the coalescence and sedimentation of the emulsion.

The silica particles in Method 3 could only be modified successfully as follows. The oil phase was prepared from mixture of 20 mL of DCM, 1g of PSF and 1.5 mL of linseed oil. An oil phase (1−4 mL) was added to the water phase (10 mL) consisting of 3 wt% Ludox TMA. Emulsification was performed via ultrasonication with a 1/8" microtip probe (Qsonica Q700-220 sonicator) for 5 min (10 s on, 5 s off pulse regime at 70% amplitude) with ice bath cooling. The polymerization of the emulsions was accomplished using the DCM solvent evaporation technique. The boiling point of DCM

is 35 °C. The DCM solvent evaporation was conducted at 32 °C for 6 h to avoid the formation of porous structures on the surface of the microcapsules. Half a millilitre of QC18 was added and stirred overnight at 20 °C on the last stage. A detailed discussion of the mechanism of the hydrolysis and condensation reactions between the QC18 and the hydroxyl groups of the silica particles is provided in a previous work [27]. A powder of microcapsules was collected via centrifugation. Figure 1 represents the overall preparation process for multifunctional microcapsules.

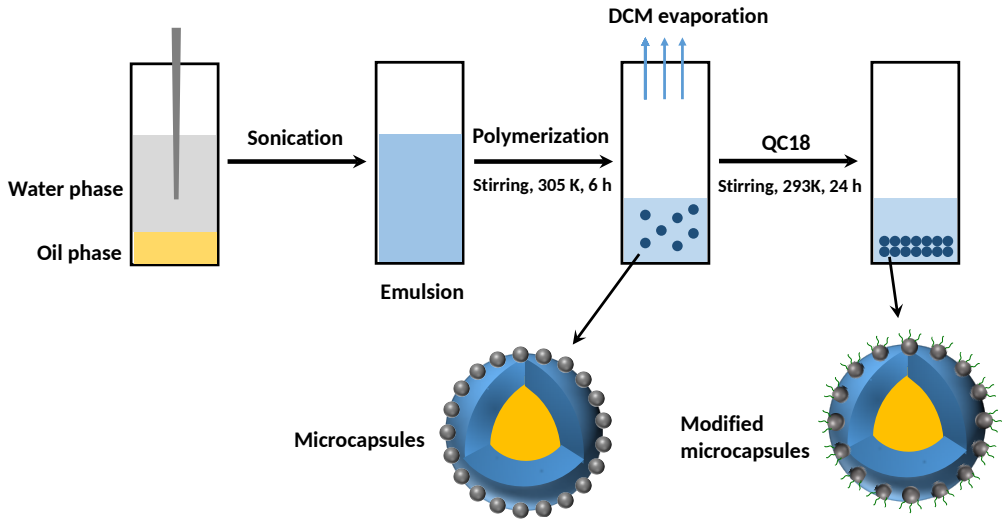

Fig. 1. Synthesis of QC18 modified microcapsules loaded with linseed oil as corrosion inhibitor.

2.3. Characterizations

Emulsion drop size distributions were determined using a Malvern Mastersizer 3000 instrument by dispersing a drop of emulsion in pure water. The optical microscopy of the emulsions involved adding a small sample to a glass plate and viewing it with a Brunel microscope fitted with a Canon EOS 1100D camera. Images were processed

using EOS Utility software. The interfacial tension of linseed oil against air, water, and Ludox TMA suspension was measured at 20 °C via the pendant the drop method using drop shape analysis system DSA10Mk2 (Krüss, Germany).

The chemical structure of linseed oil, PSF, and the resulting microcapsules was analysed via Fourier transform infrared spectroscopy (FTIR) on a Bruker TENSOR II instrument equipped with an all-reflective diamond ATR. All spectra were obtained in absorbance mode with 32 scans from 4000 cm^{-1} to 400 cm^{-1}. Thermogravimetric analysis (TGA) was performed to investigate the thermal stability of linseed oil, PSF, and the resulting microcapsules. Moreover, the analysis was performed on a Linseis microbalance (model STA PT1000) where the samples were heated at 5 °C min^{-1} from 30 °C to 800 °C under nitrogen atmosphere. The morphology of the capsules was observed using a JSM-7001F scanning electron microscope (SEM) from JEOL.

For evaluation of the self-healing performance of microcapsules in epoxy coatings, the coatings were prepared by following procedure: 5 wt% of multifunctional microcapsules was added to 5 g of bisphenol diglycidyl ether (this is the optimal concentration of the capsules in the coatings for self-healing performance according to our findings [6]). The mixture was treated by ultrasonication for 30 min. After degassing in a vacuum oven for 10 min, 5 g of trithylenetetramine was added followed by magnetic stirring for 10 min. Lastly, the composite coatings were applied on carbon steel electrodes using a bar coater. The coated electrodes were cured under room temperature for 48 h and then placed in an oven at 50 °C for 12 h. Pure epoxy coating

was also prepared in a similar manner for comparison. The dry film thicknesses of all coatings were approximately 50 ± 5 μm, as measured with a coating thickness gauge (EC770). Prior to testing, a scratch was created on the coating surface by using a blade, exposing a 4 × 0.2 mm^2 steel substrate to the electrolyte, each crack was deep enough to reach the steel substrate.

Localized electrochemical impedance spectroscopy (LEIS) was performed to confirm the self-healing effect of microcapsules added to a traditional epoxy coating [28]. LEIS measurements were performed using a VersaSCAN microscanning electrochemical workstation (AMETEK, USA). The electrode, with a diameter of 10 μm, was set to vibrate at a speed of 200 μm/s with an amplitude of 10 mV. The impedance values were collected at the frequency of 10 Hz on an area of 5 × 5 mm^2 with 26 × 26 scanning points.

The antibacterial efficacy of the microcapsules was evaluated against Staphylococcus aureus (ATCC 25913). The culture of the bacteria was grown in LB broth (containing 5.0 g of sodium chloride, 5.0 g of Tryptone and 2.5 g of yeast extract in 500 cm^3 of distilled water) at 37 °C overnight. The optical density was adjusted to 0.1 at 600 nm and serially diluted to a concentration of 10^3 CFU/mL for use. The QC18-modified microcapsules were placed in 1 mL Eppendorf tubes at concentrations of 0.5, 1, 2, 5, 10, and 20 mg/mL. The oil-encapsulated microcapsules without any QC18 at a concentration of 5 mg/mL were used for a negative control. One millilitre of 10^3 CFU/mL bacterial solution was added to each Eppendorf tube and placed in a shaking

incubator (INCU-Line® ILS4, VWR, US) at 37 °C for 3 h. After 3 h, 10 µL aliquots of each sample solution were placed on agar, and the Miles and Misra method was used to calculate the bacterial colonies in each sample [29,30]. All samples were investigated in triplicate for statistical reason.

3. Results and discussion

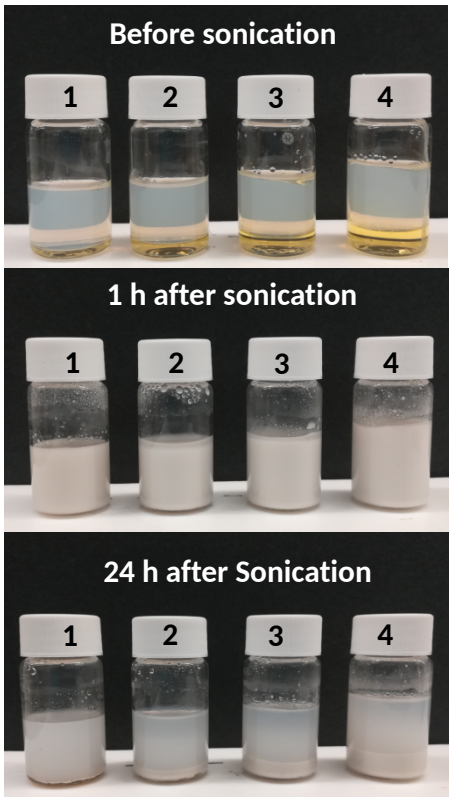

Fig. 2. Preparation of Pickering emulsions for different volume ratio of water to oil phase (1) 10:1, (2) 10:2, (3) 10:3 and (4) 10:4.

The visual images of Pickering emulsions are shown in Figure 2. Four ratios of water to oil (10:1, 10:2, 10:3, and 10:4) were considered. Two separate phases were observed before sonication. Milky solutions were observed from the photographs taken 1 h after sonication. After 24 h, the emulsion droplets sank to the bottom of the vial due to the

density difference between water and Pickering emulsion phase. The sediment height increased as the oil phase fraction increased. No linseed oil could be observed on top of the vial, indicating that all emulsions were stable against coalescence.

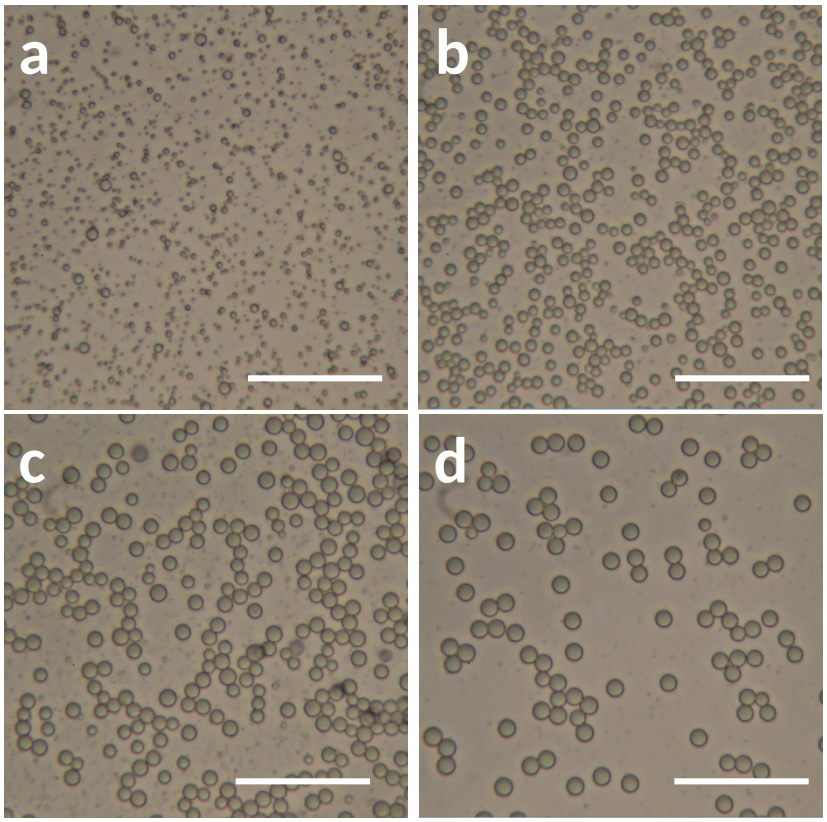

Fig. 3. Optical microscopy image of Pickering emulsions after 24 h for different volume ratio of water to oil phase (a) 10:1, (b) 10:2, (c) 10:3 and (d) 10:4. Length of unlabelled scale bar equals to 50 μm.

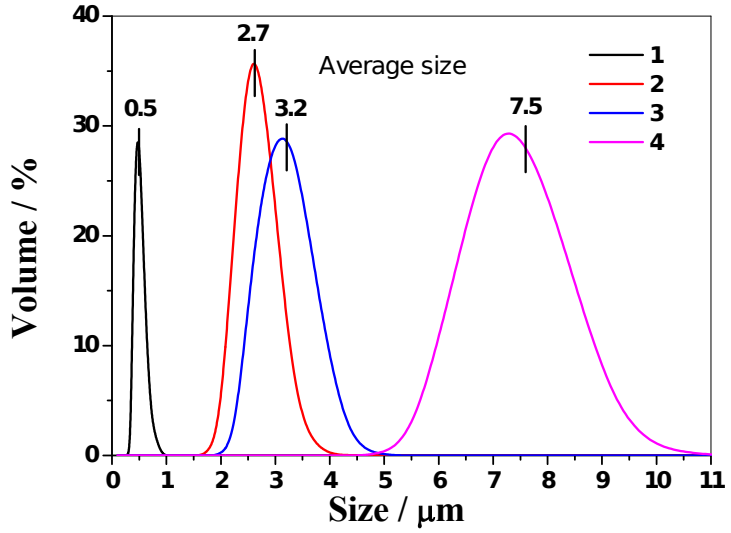

Fig. 4. Droplets size distributions for different volume ratio of water to oil phase measured by Dynamic Light Scattering (DLS): (1) 10:1, (2) 10:2, (3) 10:3 and (4) 10:4.

Optical microscopy images (Fig. 3) showed that the emulsion droplets were nicely dispersed in a continuous water phase. The average droplet size of emulsions underwent an evident change when the volume fraction of oil was varied. Additional water phases implied an increase in silica nanoparticle mass fraction. The Pickering emulsions were small when the number of particles used to stabilize the emulsion was large [21,31]. The dynamic light scattering of all emulsions was performed to provide detailed information about the size distribution of the droplets, as shown in Figure 4. The average sizes of the emulsions were 0.5, 2.7, 3.2, and 7.5 μm when the volume ratios of water to oil phase were 10:1, 10:2, 10:3, and 10:4, respectively.

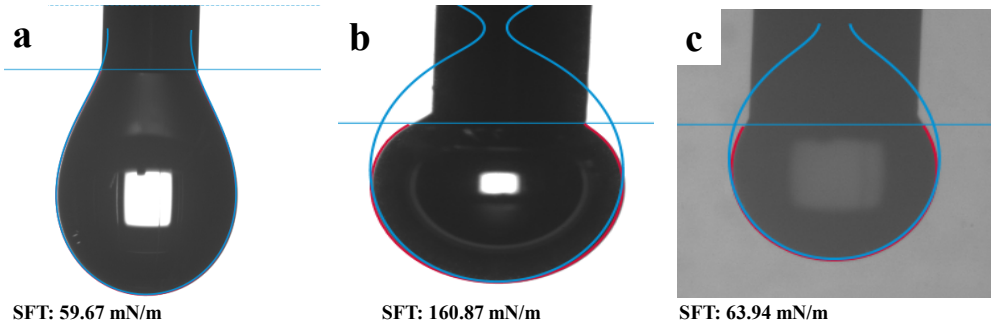

Fig. 5. Surface tension of linseed oil against air (a), water (b) and 3 wt% Ludox TMA suspension(c).

Additionally, surface tension of linseed oil against air, water, and Ludox TMA suspension was employed to confirm the stability of Pickering emulsion. In general, more hydrophilic particles can stabilize o/w emulsions and more hydrophobic particles can stabilize w/o emulsions. Grafted silica particles are often used for the stabilization of Pickering emulsions [32-34]. Justyna et al. [35] prepared a series of Pickering emulsions using fully hydrophilic silica nanoparticles and pointed out that the oil−water surface tension was a relevant criterion for oil selection. Figure 5 shows the surface tension of linseed oil against (a) air, (b) water and (c) 3 wt% Ludox TMA suspension. These pictures were taken at the instant when the biggest droplets were formed. The surface tension of linseed oil against air is 59.67 mN/m, which is lower than that of water (72.86 mN/m). Figures 5 (b) and (c) show that surface tension of linseed oil underwent a sharp decrease from 160.87 to 63.94 mN/m after 3 wt% Ludox TMA was added to the water. This reduction was attributed to the adsorbed solid particles at the oil/water interface, which provides emulsion stability.

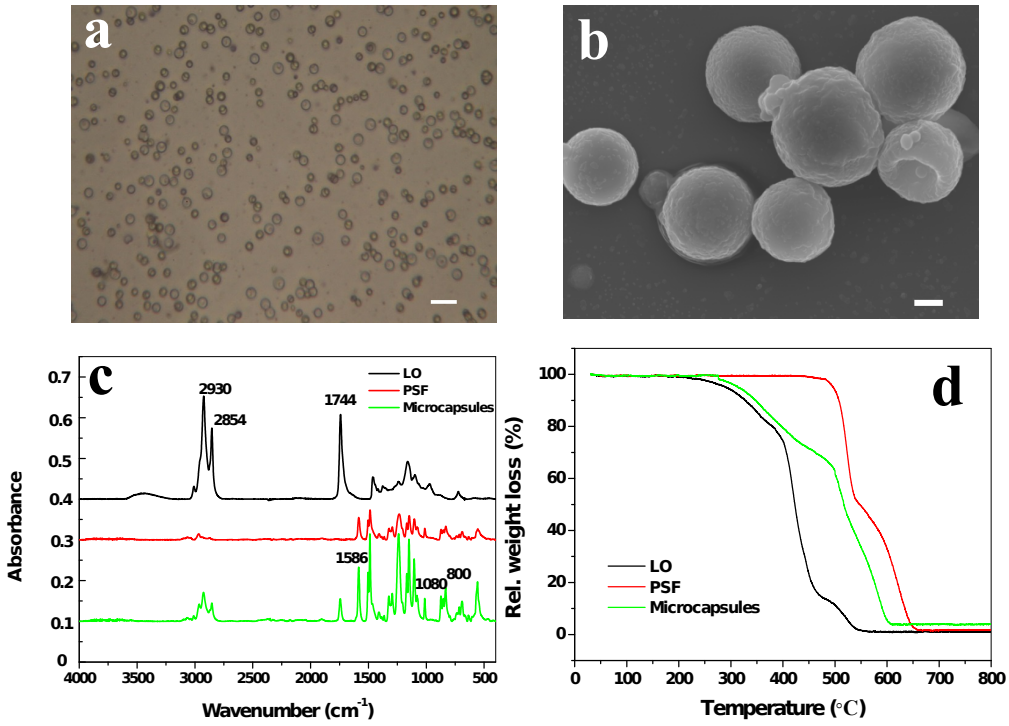

Fig. 6. (a) Optical microscopy image of microcapsules dispersed in cyclohexane (length of unlabelled scale bar equals 50 μm), (b) SEM image of microcapsules (length of unlabelled scale bar equals 1 μm), (c) ATR-FTIR spectra of linseed oil (LO), PSF, and microcapsules, (d) TGA curves for linseed oil (LO), PSF and unmodified microcapsules.

Many hydroxyl groups on the surface of microcapsules were identified before modification. These hydroxyl groups were dispersed well in water and suitable for waterborne coatings. These microcapsules aggregate together in water as most of the hydroxyl groups reacted with the QC18 after modification. Organic solvents were selected to disperse the modified microcapsules. Figure 6 (a) displays a homogeneous distribution of QC18-modified microcapsules in cyclohexane. Most of the particles maintained sufficient interparticle distances, indicating their potential application in solvent-borne coatings.

The SEM results of microcapsules are shown in Figure 6 (b). The microcapsules have a raspberry-like surface due to the silica aggregates in the shell. The image at higher magnification can be found in Figure S4 of Supporting Information section. No evidence of coalescence and collapsed structures was identified. A dimple-like structures were be found on the SEM image. This structures could be a result of the high energy beam of electrons and the vacuum condition under SEM observation. As a rough estimate, the diameter of microcapsules was approximately 4−6 μm.

To further assess the chemical structure of microcapsules, Fourier transform infrared spectroscopy and thermal gravimetric analysis of linseed oil, PSF, and modified microcapsules were carried out. The ATR-FTIR spectra of linseed oil, PSF, and modified microcapsules are presented in Figure 6 (c). The absorption peaks at 2930, 2854, 1744, and 1458 cm^{-1} correspond to =C−H stretching, C−H stretching, C=O stretching, and C−H bending, respectively. All these peaks are characteristic for linseed oil [36]. The spectrum of PSF shows characteristic peaks at 1489, 1504, 1586 cm^{-1} (C=C aromatic rings stretching), 1323, 1295 cm^{-1} (O=S=O asymmetric stretching), and 1230 cm^{-1} (C-O-C asymmetric stretching) [25]. The spectrum of filled microcapsules displays the characteristic peaks of linseed oil and the absorption band characteristics of the PSF. The absorption peaks at 800 and 1080 cm^{-1} correspond to Si−O−Si symmetric stretching and Si−O asymmetric vibration, respectively. All these peaks are characteristics of SiO_2. The ATR-FTIR results confirmed the successful encapsulation of linseed oil in microcapsules. Furthermore, no broad –OH peak at approximately 3400

cm^{-1} was identified because most of the hydroxyl groups reacted with QC18. The nanoparticles on the surface of the microcapsules have a Janus-like structure, as shown in Figure 1, with one side embedded inside the shell and the other side modified with QC18, which rendered the microcapsule antibacterial function.

The TGA curves of unmodified microcapsules, linseed oil, and PSF were obtained from 30 ºC to 800 ºC under N_2 protection to determine the loading capacity of microcapsules. As shown in Figure 6 (d), the decomposition of pristine linseed oil started at 300 ºC with a fast weight loss rate between 400 ºC and 450 ºC [37]. Decomposition stopped at 540 ºC without any residues. The PSF started to decompose at 500 ºC and finished at 650 ºC [25]. The TGA curve of unmodified microcapsules could be divided into two parts. The 40 wt% weight loss of microcapsules is mainly attributed to the calcination of linseed oil between 300 ºC to 500 ºC. The remaining mass was lost from 500 ºC to 600 ºC due to linseed and PSF decomposition. Results from the TGA analysis confirmed that at least 40 wt% of linseed oil was encapsulated in the microcapsules.

Localized electrochemical impedance spectroscopy (LEIS) were carried out to confirm the self-healing effect provided by the microcapsules. Compared with conventional electrochemical impedance spectroscopy (EIS), LEIS provides more detailed information about the corrosion inhibition effect and self-healing mechanisms in a localized manner [38-41]. The EIS convolutes the separate responses of the coating and defect together; however, this convolution is not relevant if the focus is on the local self-healing effect of the coating. LEIS, which commonly uses a five-electrode

configuration, is based on the ratio of the applied AC voltage to the local AC current density (i_{local}). i_{local} is calculated in accordance with the Ohm's law (1), where d is the distance between the two probes, and κ is the conductivity of the electrolyte.

$$i_{local} = \frac{\Delta V_{local}}{d} \kappa \quad (1)$$

The local admittance is calculated by equation (2), where the applied voltage ($\Delta V_{applied}$) is the potential difference between the reference electrode and the working electrode [42].

$$Y_{local} = \frac{i_{local}}{\Delta V_{applied}} \quad (2)$$

Figure 7 shows the admittance mapping of the scratched coatings; the mapping was obtained in 3.5 wt% NaCl solution at different times of immersion up to 24 h. A low frequency (10 Hz) was selected because it can exhibit the self-healing process of scratched coatings fast and effectively [43]. After 3 h, the defect was evident in Figure 7 (a) on the micrograph and reflected in the admittance map as a large increase around the scratched area. The defect remains active for 24 h. The intelligent coating behaves completely different. No remarkable increase in the admittance in the defect zone was observed during the entire test period. This effect is responsible for the reduction of the corrosion activity of the substrate due to the release of linseed oil. Linseed oil forms a solid film through chemical reaction with oxygen, which has been used as a healing agent for many years [37,44]. In order to verify the results of LEIS, the tested samples

were observed through optical microscopy after removing coatings (Figure S5). In the case of the steel coated with intelligent coating (Figure S5 (b)), small corrosion area proves their self-healing functionality and better barrier properties. This is in accordance with the LEIS test.

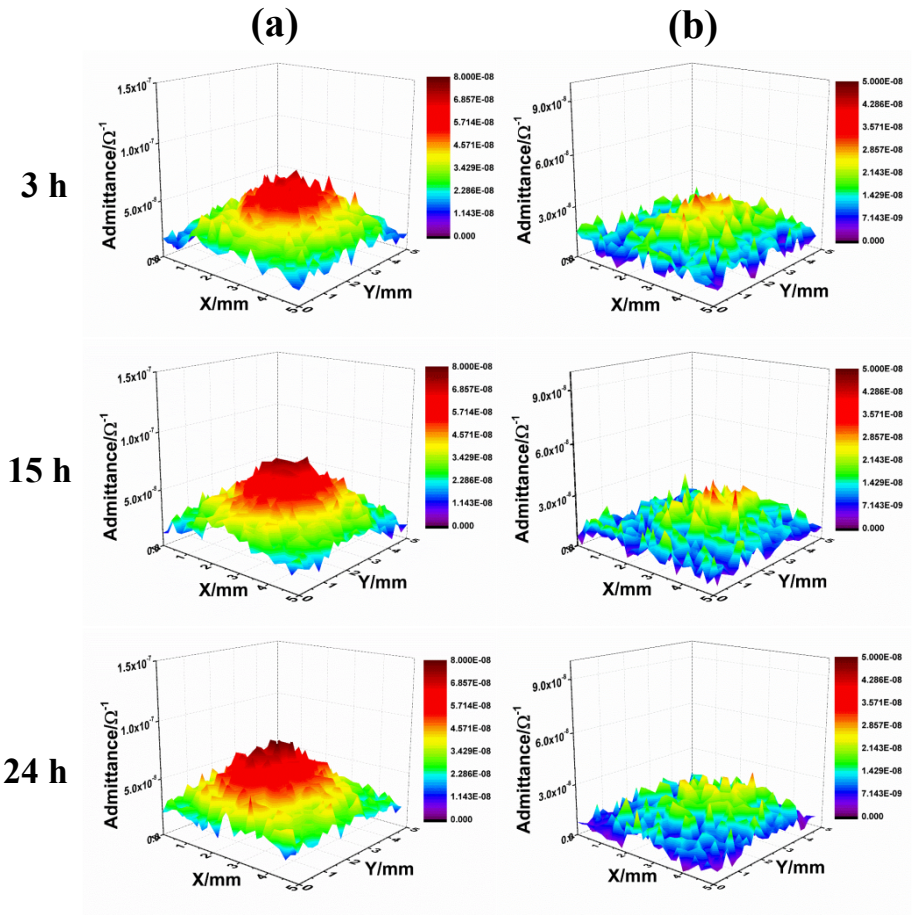

Fig. 7. Local admittance mappings performed at 10 Hz over the scratch after 3 h, 15 h and 24 h of immersion in 3.5 wt% NaCl for: (a) controlled coatings and (b) intelligent coating.

The second, antimicrobial effect of the microcapsules was demonstrated by the antibacterial experiments. The antibacterial efficacy of the QC18-modified capsules was evaluated against Gram-positive S. aureus and is presented in Figure 8(a). The photographs of the agar plates are given in Figure 8(b). The positive control sample was just the oil-encapsulated capsules without the presence of an active antimicrobial. All concentrations of the QC18-modofied capsules displayed antibacterial activity, which increased from QC18-oil0.5 sample showing an antimicrobial efficacy of 52% for the 5 and 10 mg/mL samples showing over 90% antimicrobial efficacy. Increasing the capsules' concentration further to 20 mg/mL decreased the antimicrobial efficacy to 86%. QC18 molecules tethered to the MSN particles killed the bacteria by interacting with the lipid bilayer structures of microbial cell membranes, thereby causing leakage and cell death.

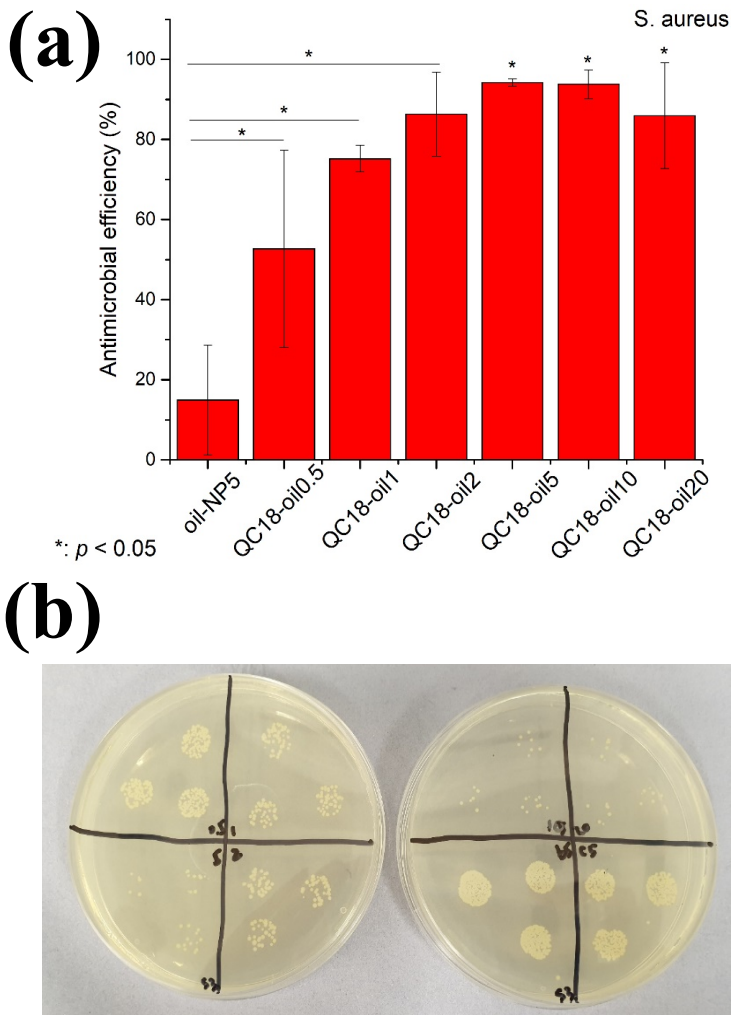

Fig. 8. (a) S.aureus inhibition efficiency of QC18 modified capsules (0.5, 1, 2, 5, 10, 20 mg/ml) and oil-encapsulated capsules (5mg/ml, as control group) after 3 h shaking incubation. (b) CFU agar plate read of QC18 modified capsules (0.5, 1, 2, 5, 10, 20 mg/ml) and oil-encapsulated capsules (5mg/ml, as control group) after 3 h shaking incubation. Presentative CFU image is the third run of the tests.

4. Conclusions

A novel type of microcapsule prepared via Pickering emulsion polymerization based on linseed oil-filled polysulfone/QC18-modified silica hybrid shell was reported. The chemical structure of microcapsules was confirmed via Fourier transform infrared spectroscopy and thermal gravimetric analysis. The microcapsules were embedded into an epoxy coating. The hybrid coating exhibited remarkable self-healing effect in the

scratched area filling it with polymer film formed by reaction of encapsulated linseed oil and atmospheric oxygen. A significant advantage compared to the other types of previously developed micro/nanocapsules is their outer surface modified by QC18, thus providing stable antimicrobial effect. This work paves a way for researchers to explore various multifunctional micro/nanocontainers, which can be obtained by choosing among various antimicrobial or anticorrosion agents. The ongoing research is focused on assessing the coatings under real seawater conditions to demonstrate the multifunctional micro/nanocontainers in actual industrial applications.

Declaration of Competing Interest

The authors declare no conflict of interest.

Acknowledgments

The authors are grateful for the financial support provided by Natural Science Foundation of China (51801110), Shandong Province Natural Science Foundation, China (ZR2017BD038, ZR2016DM21). The work was supported by ERC grant ENERCAPSULE (#647969). VV, PK and DS thank financial support from Russian Science Foundation (grant 19-79-30091) provided for antifouling and anticorrosion measurements.

References

[1] Y. Dong, Y. Lekbach, Z. Li, D. Xu, S. El Abed, S. Ibnsouda Koraichi, F. Wang, Microbiologically influenced corrosion of 304L stainless steel caused by an alga associated bacterium Halomonas titanicae, Journal of Materials Science & Technology 37 (2020) 200-206.

[2] Y. Li, C. Ning, Latest research progress of marine microbiological corrosion and bio-fouling, and new approaches of marine anti-corrosion and anti-fouling, Bioactive Materials 4 (2019) 189-195.
[3] G. Sun, H. Ge, J. Luo, R. Liu, Highly wear-resistant UV-curing antibacterial coatings via nanoparticle self-migration to the top surface, Prog. Org. Coat. 135 (2019) 19-26.
[4] W. Zhang, J.-X. Li, R.-C. Tang, A.-D. Zhai, Hydrophilic and antibacterial surface functionalization of polyamide fabric by coating with polylysine biomolecule, Prog. Org. Coat. 142 (2020) 105571.
[5] Y. Zhao, E. Zhou, D. Xu, Y. Yang, Y. Zhao, T. Zhang, T. Gu, K. Yang, F. Wang, Laboratory investigation of microbiologically influenced corrosion of 2205 duplex stainless steel by marine Pseudomonas aeruginosa biofilm using electrochemical noise, Corros. Sci. 143 (2018) 281-291.
[6] D.G. Shchukin, H. Möhwald, A Coat of Many Functions, Science 341 (2013) 1458-1459.
[7] K. S. Toohey, N. R. Sottos, J. A. Lewis, J. S. Moore, S. R. White, Self-healing materials with microvascular networks, Nat. Mater. 6 (2007) 581.
[8] S. R. White, N. R. Sottos, P. H. Geubelle, J. S. Moore, M. R. Kessler, S. R. Sriram, E. N. Brown, S. Viswanathan, Autonomic healing of polymer composites, Nature 409 (2001) 794-797.
[9] D. V. Andreeva, D. Fix, H. Möhwald, D. G. Shchukin, Self-Healing Anticorrosion Coatings Based on pH-Sensitive Polyelectrolyte/Inhibitor Sandwichlike Nanostructures, Adv. Mater. 20 (2008) 2789-2794.
[10] S. V. Lamaka, D. G. Shchukin, D. V. Andreeva, M. L. Zheludkevich, H. Möhwald, M. G. S. Ferreira, Sol-Gel/Polyelectrolyte Active Corrosion Protection System, Adv. Funct. Mater. 18 (2008) 3137-3147.
[11] D. G. Shchukin, H. Möhwald, Surface-Engineered Nanocontainers for Entrapment of Corrosion Inhibitors, Adv. Funct. Mater. 17 (2007) 1451-1458.
[12] D. G. Shchukin, M. Zheludkevich, K. Yasakau, S. Lamaka, M. G. S. Ferreira, H. Möhwald, Layer-by-Layer Assembled Nanocontainers for Self-Healing Corrosion Protection, Adv. Mater. 18 (2006) 1672-1678.
[13] M. L. Zheludkevich, D. G. Shchukin, K. A. Yasakau, H. Möhwald, M. G. S. Ferreira, Anticorrosion Coatings with Self-Healing Effect Based on Nanocontainers Impregnated with Corrosion Inhibitor, Chem. Mater. 19 (2007) 402-411.
[14] Z. Zheng, X. Huang, M. Schenderlein, D. Borisova, R. Cao, H. Möhwald, D. Shchukin, Self-Healing and Antifouling Multifunctional Coatings Based on pH and Sulfide Ion Sensitive Nanocontainers, Adv. Funct. Mater. 23 (2013) 3307-3314.
[15] E. Shchukina, D. G. Shchukin, Nanocontainer-Based Active Systems: From Self-Healing Coatings to Thermal Energy Storage, Langmuir (2019).
[16] E. Shchukina, H. Wang, D. G. Shchukin, Nanocontainer-based self-healing coatings: current progress and future perspectives, Chem. Commun. 55 (2019) 3859-3867.
[17] F. Zhang, P. Ju, M. Pan, D. Zhang, Y. Huang, G. Li, X. Li, Self-healing mechanisms in smart protective coatings: A review, Corros. Sci. 144 (2018) 74-88.
[18] B. Qian, Z. Song, L. Hao, W. Wang, D. Kong, Self-Healing Epoxy Coatings Based on Nanocontainers for Corrosion Protection of Mild Steel, J. Electrochem. Soc. 164 (2017) C54-C60.

[19] B. Qian, Z. Zheng, M. Michailids, N. Fleck, M. Bilton, Y. Song, G. Li, D. Shchukin, Mussel-Inspired Self-Healing Coatings Based on Polydopamine-Coated Nanocontainers for Corrosion Protection, ACS Appl. Mater. Interfaces 11 (2019) 10283-10291.
[20] S. U. Pickering, CXCVI.—Emulsions, J. Am. Chem. Soc. 91 (1907) 2001-2021.
[21] B. P. Binks, Particles as surfactants—similarities and differences, Curr. Opin. Colloid Interface Sci. 7 (2002) 21-41.
[22] B. P. Binks, S. O. Lumsdon, Stability of oil-in-water emulsions stabilised by silica particles, Phys. Chem. Chem. Phys. 1 (1999) 3007-3016.
[23] M. F. Haase, D. O. Grigoriev, H. Möhwald, D. G. Shchukin, Development of Nanoparticle Stabilized Polymer Nanocontainers with High Content of the Encapsulated Active Agent and Their Application in Water-Borne Anticorrosive Coatings, Adv. Mater. 24 (2012) 2429-2435.
[24] M. F. Haase, D. Grigoriev, H. Moehwald, B. Tiersch, D. G. Shchukin, Encapsulation of Amphoteric Substances in a pH-Sensitive Pickering Emulsion, J. Phys. Chem. C 114 (2010) 17304-17310.
[25] H. Li, S. Li, Z. Li, Y. Zhu, H. Wang, Polysulfone/SiO2 Hybrid Shell Microcapsules Synthesized by the Combination of Pickering Emulsification and the Solvent Evaporation Technique and Their Application in Self-Lubricating Composites, Langmuir 33 (2017) 14149-14155.
[26] M. Tischer, G. Pradel, K. Ohlsen, U. Holzgrabe, Quaternary Ammonium Salts and Their Antimicrobial Potential: Targets or Nonspecific Interactions?, Chemmedchem 7 (2012) 22-31.
[27] M. Michailidis, I. Sorzabal-Bellido, E. A. Adamidou, Y. A. Diaz-Fernandez, J. Aveyard, R. Wengier, D. Grigoriev, R. Raval, Y. Benayahu, R. A. D'Sa, D. Shchukin, Modified Mesoporous Silica Nanoparticles with a Dual Synergetic Antibacterial Effect, ACS Appl. Mater. Interfaces 9 (2017) 38364-38372.
[28] C. Liu, H. Zhao, P. Hou, B. Qian, X. Wang, C. Guo, L. Wang, Efficient Graphene/Cyclodextrin-Based Nanocontainer: Synthesis and Host–Guest Inclusion for Self-Healing Anticorrosion Application, ACS Appl. Mater. Interfaces 10 (2018) 36229-36239.
[29] A. A. Miles, S. S. Misra, J. O. Irwin, The estimation of the bactericidal power of the blood, Epidemiol. Infect. 38 (2009) 732-749.
[30] G. Fleming, J. Aveyard, J. L. Fothergill, F. McBride, R. Raval, R. A. D'Sa, Nitric Oxide Releasing Polymeric Coatings for the Prevention of Biofilm Formation, Polymers 9 (2017) 601.
[31] R. Aveyard, B. P. Binks, J. H. Clint, Emulsions stabilised solely by colloidal particles, Adv. Colloid Interface Sci. 100-102 (2003) 503-546.
[32] B. P. Binks, J. A. Rodrigues, Types of Phase Inversion of Silica Particle Stabilized Emulsions Containing Triglyceride Oil, Langmuir 19 (2003) 4905-4912.
[33] B. P. Binks, J. H. Clint, Solid Wettability from Surface Energy Components: Relevance to Pickering Emulsions, Langmuir 18 (2002) 1270-1273.
[34] A. Schoth, K. Landfester, R. Muñoz-Espí, Surfactant-Free Polyurethane Nanocapsules via Inverse Pickering Miniemulsion, Langmuir 31 (2015) 3784-3788.
[35] J. Frelichowska, M.-A. Bolzinger, Y. Chevalier, Pickering emulsions with bare silica, Colloids Surf., A 343 (2009) 70-74.

[36] D. A. Leal, I. C. Riegel-Vidotti, M. G. S. Ferreira, C. E. B. Marino, Smart coating based on double stimuli-responsive microcapsules containing linseed oil and benzotriazole for active corrosion protection, Corros. Sci. 130 (2018) 56-63.
[37] C. Suryanarayana, K. C. Rao, D. Kumar, Preparation and characterization of microcapsules containing linseed oil and its use in self-healing coatings, Prog. Org. Coat. 63 (2008) 72-78.
[38] F. Zou, D. Thierry, Localized electrochemical impedance spectroscopy for studying the degradation of organic coatings, Electrochim. Acta 42 (1997) 3293-3301.
[39] J.-B. Jorcin, H. Krawiec, N. Pébère, V. Vignal, Comparison of local electrochemical impedance measurements derived from bi-electrode and microcapillary techniques, Electrochim. Acta 54 (2009) 5775-5781.
[40] M. W. Wittmann, R. B. Leggat, S. R. Taylor, The Detection and Mapping of Defects in Organic Coatings Using Local Electrochemical Impedance Methods, J. Electrochem. Soc. 146 (1999) 4071-4075.
[41] J. V. Nardeli, D. V. Snihirova, C. S. Fugivara, M. F. Montemor, E. R. P. Pinto, Y. Messaddecq, A. V. Benedetti, Localised corrosion assessement of crambe-oil-based polyurethane coatings applied on the ASTM 1200 aluminum alloy, Corros. Sci. 111 (2016) 422-435.
[42] L. V. S. Philippe, G. W. Walter, S. B. Lyon, Investigating Localized Degradation of Organic Coatings: Comparison of Electrochemical Impedance Spectroscopy with Local Electrochemical Impedance Spectroscopy, J. Electrochem. Soc. 150 (2003) B111-B119.
[43] A. S. Nguyen, N. Pébère, A local electrochemical impedance study of the self-healing properties of waterborne coatings on 2024 aluminium alloy, Electrochim. Acta 222 (2016) 1806-1817.
[44] M. Lazzari, O. Chiantore, Drying and oxidative degradation of linseed oil, Polym. Degrad. Stab. 65 (1999) 303-313.

TOC Graphic

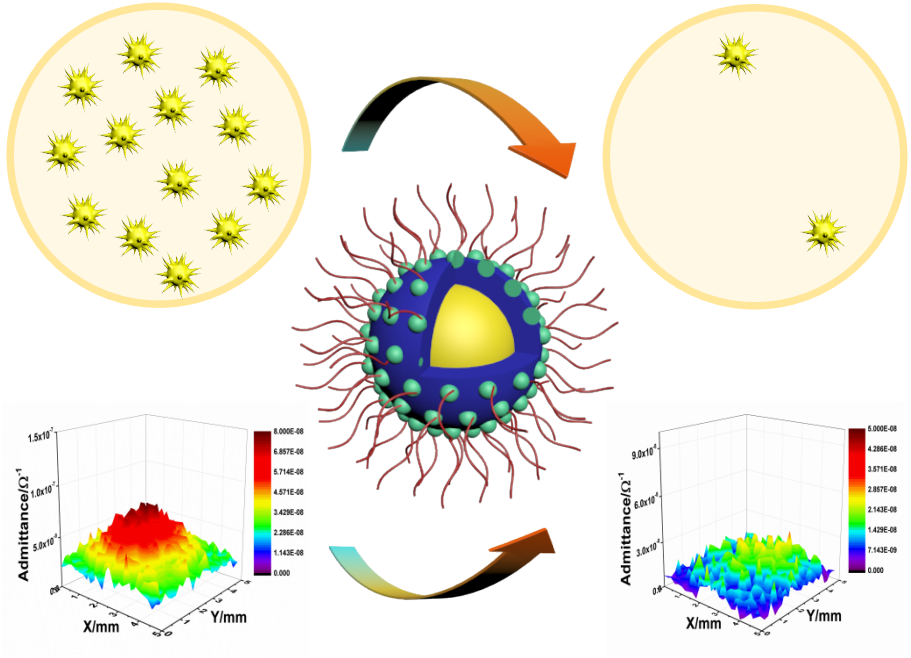

Microcapsules Prepared via Pickering Emulsion Polymerization for Multifunctional Coatings

Bei Qian[a, b], Zhaoliang Zheng[b], Chengbao Liu[c], Man Li[d], Raechelle A. D'Sa[d], Haiyan Li[b], Michael Graham[b], Marios Michailidis[b], Pavel Kantserev[e], Vladimir Vinokurov[e], Dmitry Shchukin[b, e*]

[a] *College of Chemistry and Pharmaceutical Sciences, Qingdao Agricultural University, 700 Changcheng Road, Qingdao 266109, PR China.*

[b] *Stephenson Institute for Renewable Energy, Department of Chemistry, University of Liverpool, Crown Street, Liverpool L69 7ZD, U.K.*

[c] *Ningbo Institute of Materials Technology and Engineering, Chinese Academy of Science, Ningbo 315201, China.*

[d] *Department of Mechanical, Materials and Aerospace Engineering, University of Liverpool, Liverpool L69 3GH, U.K.*

[e] *Gubkin University, 19991, Russia, Moscow, 65/1 Leninsky prospect.*

Corresponding author: Prof. Dmitry Shchukin

Stephenson Institute for Renewable Energy, Department of Chemistry, University of Liverpool, Crown Street, Liverpool L69 7ZD, U.K.

E-mail: D.Shchukin@liverpool.ac.uk

Tel.: 0044-151-7952304

Research Highlights

1. Microcapsules with antimicrobial shell and anticorrosion core were prepared.

2. Linseed oil in water emulsion were stabilized by hydrophilic silica nanoparticles.

3. QC18-modified microcapsules provide additional antibacterial performance.

4. LEIS results exhibited remarkable self-healing effect of hybrid coating.

5. Microcapsules showed >90 % antimicrobial efficacy against Gram-positive S. aureus.

Microcapsules Prepared via Pickering Emulsion Polymerization for Multifunctional Coatings

Bei Qian[a, b], Zhaoliang Zheng[b], Chengbao Liu[c], Man Li[d], Raechelle A. D'Sa[d], Haiyan Li[b], Michael Graham[b], Marios Michailidis[b], Pavel Kantserev[e], Vladimir Vinokurov[e], Dmitry Shchukin[b, e*]

[a] *College of Chemistry and Pharmaceutical Sciences, Qingdao Agricultural University, 700 Changcheng Road, Qingdao 266109, PR China.*

[b] *Stephenson Institute for Renewable Energy, Department of Chemistry, University of Liverpool, Crown Street, Liverpool L69 7ZD, U.K.*

[c] *Ningbo Institute of Materials Technology and Engineering, Chinese Academy of Science, Ningbo 315201, China.*

[d] *Department of Mechanical, Materials and Aerospace Engineering, University of Liverpool, Liverpool L69 3GH, U.K.*

[e] *Gubkin University, 19991, 65/1 Leninsky prospect, Moscow, Russia.*

Keywords: Pickering emulsion; self-healing; antimicrobial; localized electrochemical impedance spectroscopy

Abstract: Micro/nanocontainer-based self-healing coatings have achieved enormous interest in scientific community during the last decade. However, the search for multifunctional micro/nanocontainers still has research challenge, especially for the micro/nanocontainers with dual functionality (both anticorrosion and antimicrobial). Here, a novel type of microcapsules with antimicrobial shell and anticorrosion core was prepared by the Pickering emulsion polymerization technique. Dimethyloctadecyl [3-(trimethoxysilyl) propyl] ammonium chloride (QC18) and linseed oil were encapsulated as the antimicrobial and the anticorrosion agents, respectively. The results of local electrochemical impedance spectroscopy (LEIS) at 10 Hz demonstrated corrosion suppression in the scratched area of coatings doped with multifunctional microcapsules. Additionally, the QC18-modified microcapsules exhibited high antibacterial performance, showing over 90 % antimicrobial efficacy against gram-positive bacteria. This type of dual-functional coating might guide future design of micro/nanocontainer-based self-healing paint formulations.

1. Introduction

The cost of marine corrosion is increasing every year. The National Association of Corrosion Engineers (NACE)'s IMPACT study has estimated that the total cost of marine corrosion worldwide is between $50 and $80 billion every year. In addition to this intrinsic properties of seawater (e.g., chloride content, efficient electrolyte, and splash zones), microorganism-induced corrosion (MIC) also causes the deterioration of

metallic structures. A large part of the economic losses in the marine industry is caused by MIC [1-5].

Isolating the corroding metal from the seawater through intact coating is one of the main methods for controlling the corrosion of metals in seawater. However, the coating's barrier effects against corrosion are jeopardized due to mechanical vulnerability during transportation or service [6]. The self-healing coatings that possess rapid feedback activity in response to these attacks is a prospective solution [7,8]. After some pioneering works by the authors of this study [9-14], research related to self-healing coatings has gained tremendous attention in the recent decades [15-17]. Majority of these previous works had only focused on the anticorrosion property of the coatings. As previously mentioned, MIC should not be ignored when marine corrosion is discussed. Thus, endowing self-healing coatings with anticorrosion and antibacterial properties is interesting.

Different encapsulation methods have been used to fabricate micro/nanocapsules filled with inhibitors or active agents [18,19]; such methods can endow the coatings with intelligent self-healing properties. Polymerization is a well-established method for the fabrication of micro/nanocapsules [8]. Pickering emulsions are stabilized by solid colloidal particles, which act as emulsifiers at the oil/water interface [20]. The type of emulsion can be determined by the three-phase angle θ_{ow}. Oil-in-water (o/w) emulsions prefer hydrophilic particles ($\theta_{ow} < 90^{o}$), whereas stable inversion emulsions (w/o) are usually obtained by hydrophobic particles ($\theta_{ow} > 90^{o}$) [21,22]. Compared with the

particle's thermal energy, extremely higher energy is needed to remove it from the interface. Pickering emulsions are fantastic precursors to the formation of micro/nanocapsules from the environmental aspects. Moreover, the surface of the Pickering reservoirs can be modified by functional molecules because their shell has the properties of pure nanoparticles [23]. This feature fulfils the aforementioned requirements for multifunctional coatings.

The present study focuses on a new type of micro/nanocapsules based on Pickering emulsions with dual self-healing and antibacterial functions. In our previous works, Pickering nanocontainers in a water-based anticorrosive coating were introduced [23,24]. Polysulfone (PSF)/SiO_2 hybrid capsules were prepared using linseed oil as a core material for self-healing anticorrosion effect and surface-modified Ludox TMA particles as a stabilizer. This easy-to-operate microencapsulation method was developed to prepare the self-lubricating composites in the previous work [25]. The quaternary ammonium salts were used to make the surface of silica particles active as antibacterial agents, which can be adsorbed on the negatively charged bacterial cell membranes, leading to cell death [26].

2. Experimental section

2.1. Materials

Ludox TMA suspension (silica, 34 wt % suspension in H_2O, particle size of 22 nm, surface area 180 m^2/g), linseed oil (0.93 g/mL), PSF (1.24 g/mL) and dichloromethane

(DCM) (≥ 99.8%, 1.325 g/mL) were purchased from Sigma-Aldrich UK. Dimethyloctadecyl [3-(trimethoxysilyl) propyl] ammonium chloride (QC18, 60% in methanol) was purchased from Acros Organics. Bisphenol diglycidyl either ($C_{21}H_{24}O_4$, 1.17 g/mL) and trithylenetetramine ($C_6H_{18}N_4$, 0.98 g/mL) curing agent were purchased from Alfa Aesar. The carbon steel electrodes with an area of 1 cm^2 were polished by 400 and 800 sand papers and cleaned in acetone and ethanol using ultrasonic treatment. Staphylococcus aureus (ATCC 29213 strain), LB broth and LB agar broth were purchased from Sigma. Deionized water was used throughout the study.

2.2. Preparation of microcapsules

Three methods were used to prepare modified Pickering microcapsules encapsulated with linseed oil. Silica was modified by QC18 before emulsification (Method 1), after emulsification (Method 2), and after polymerization (Method 3). The details of Methods 1 and 2 are described in the Supporting Information. Either Method 1 or 2 failed due to the coalescence and sedimentation of the emulsion.

The silica particles in Method 3 could only be modified successfully as follows. The oil phase was prepared from mixture of 20 mL of DCM, 1g of PSF and 1.5 mL of linseed oil. An oil phase (1−4 mL) was added to the water phase (10 mL) consisting of 3 wt% Ludox TMA. Emulsification was performed via ultrasonication with a 1/8" microtip probe (Qsonica Q700-220 sonicator) for 5 min (10 s on, 5 s off pulse regime at 70% amplitude) with ice bath cooling. The polymerization of the emulsions was accomplished using the DCM solvent evaporation technique. The boiling point of DCM

is 35 °C. The DCM solvent evaporation was conducted at 32 °C for 6 h to avoid the formation of porous structures on the surface of the microcapsules. Half a millilitre of QC18 was added and stirred overnight at 20 °C on the last stage. A detailed discussion of the mechanism of the hydrolysis and condensation reactions between the QC18 and the hydroxyl groups of the silica particles is provided in a previous work [27]. A powder of microcapsules was collected via centrifugation. Figure 1 represents the overall preparation process for multifunctional microcapsules.

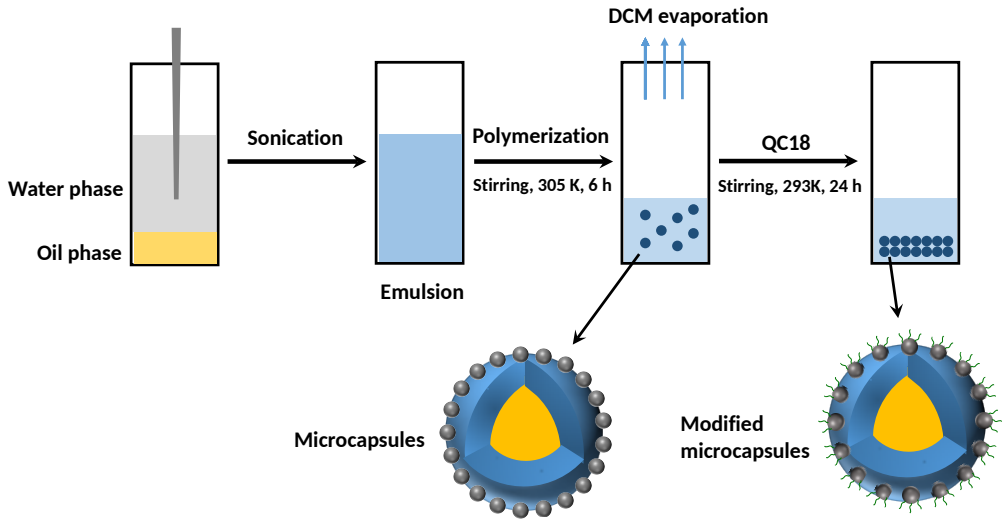

Fig. 1. Synthesis of QC18 modified microcapsules loaded with linseed oil as corrosion inhibitor.

2.3. Characterizations

Emulsion drop size distributions were determined using a Malvern Mastersizer 3000 instrument by dispersing a drop of emulsion in pure water. The optical microscopy of the emulsions involved adding a small sample to a glass plate and viewing it with a Brunel microscope fitted with a Canon EOS 1100D camera. Images were processed

using EOS Utility software. The interfacial tension of linseed oil against air, water, and Ludox TMA suspension was measured at 20 °C via the pendant the drop method using drop shape analysis system DSA10Mk2 (Krüss, Germany).

The chemical structure of linseed oil, PSF, and the resulting microcapsules was analysed via Fourier transform infrared spectroscopy (FTIR) on a Bruker TENSOR II instrument equipped with an all-reflective diamond ATR. All spectra were obtained in absorbance mode with 32 scans from 4000 cm^{-1} to 400 cm^{-1}. Thermogravimetric analysis (TGA) was performed to investigate the thermal stability of linseed oil, PSF, and the resulting microcapsules. Moreover, the analysis was performed on a Linseis microbalance (model STA PT1000) where the samples were heated at 5 °C min^{-1} from 30 °C to 800 °C under nitrogen atmosphere. The morphology of the capsules was observed using a JSM-7001F scanning electron microscope (SEM) from JEOL.

For evaluation of the self-healing performance of microcapsules in epoxy coatings, the coatings were prepared by following procedure: 5 wt% of multifunctional microcapsules was added to 5 g of bisphenol diglycidyl ether (this is the optimal concentration of the capsules in the coatings for self-healing performance according to our findings [6]). The mixture was treated by ultrasonication for 30 min. After degassing in a vacuum oven for 10 min, 5 g of trithylenetetramine was added followed by magnetic stirring for 10 min. Lastly, the composite coatings were applied on carbon steel electrodes using a bar coater. The coated electrodes were cured under room temperature for 48 h and then placed in an oven at 50 °C for 12 h. Pure epoxy coating

was also prepared in a similar manner for comparison. The dry film thicknesses of all coatings were approximately 50 ± 5 μm, as measured with a coating thickness gauge (EC770). Prior to testing, a scratch was created on the coating surface by using a blade, exposing a 4×0.2 mm^2 steel substrate to the electrolyte, each crack was deep enough to reach the steel substrate.

Localized electrochemical impedance spectroscopy (LEIS) was performed to confirm the self-healing effect of microcapsules added to a traditional epoxy coating [28]. LEIS measurements were performed using a VersaSCAN microscanning electrochemical workstation (AMETEK, USA). The electrode, with a diameter of 10 μm, was set to vibrate at a speed of 200 μm/s with an amplitude of 10 mV. The impedance values were collected at the frequency of 10 Hz on an area of 5 × 5 mm^2 with 26 × 26 scanning points.

The antibacterial efficacy of the microcapsules was evaluated against Staphylococcus aureus (ATCC 25913). The culture of the bacteria was grown in LB broth (containing 5.0 g of sodium chloride, 5.0 g of Tryptone and 2.5 g of yeast extract in 500 cm^3 of distilled water) at 37 °C overnight. The optical density was adjusted to 0.1 at 600 nm and serially diluted to a concentration of 10^3 CFU/mL for use. The QC18-modified microcapsules were placed in 1 mL Eppendorf tubes at concentrations of 0.5, 1, 2, 5, 10, and 20 mg/mL. The oil-encapsulated microcapsules without any QC18 at a concentration of 5 mg/mL were used for a negative control. One millilitre of 10^3 CFU/mL bacterial solution was added to each Eppendorf tube and placed in a shaking

incubator (INCU-Line® ILS4, VWR, US) at 37 °C for 3 h. After 3 h, 10 µL aliquots of each sample solution were placed on agar, and the Miles and Misra method was used to calculate the bacterial colonies in each sample [29,30]. All samples were investigated in triplicate for statistical reason.

3. Results and discussion

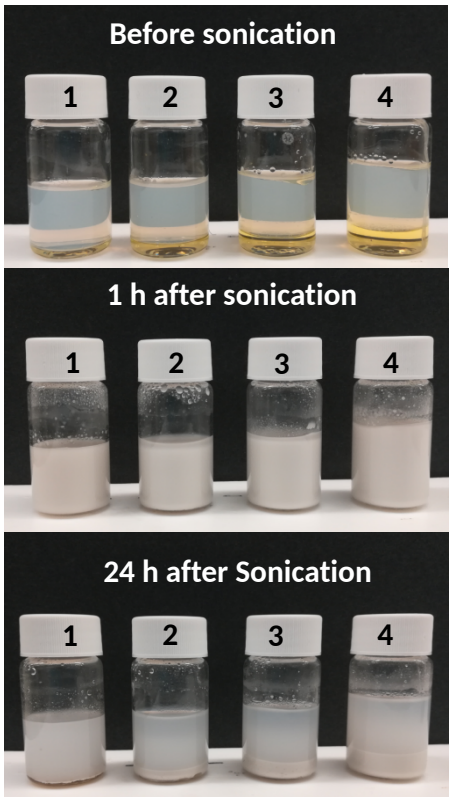

Fig. 2. Preparation of Pickering emulsions for different volume ratio of water to oil phase (1) 10:1, (2) 10:2, (3) 10:3 and (4) 10:4.

The visual images of Pickering emulsions are shown in Figure 2. Four ratios of water to oil (10:1, 10:2, 10:3, and 10:4) were considered. Two separate phases were observed before sonication. Milky solutions were observed from the photographs taken 1 h after sonication. After 24 h, the emulsion droplets sank to the bottom of the vial due to the

density difference between water and Pickering emulsion phase. The sediment height increased as the oil phase fraction increased. No linseed oil could be observed on top of the vial, indicating that all emulsions were stable against coalescence.

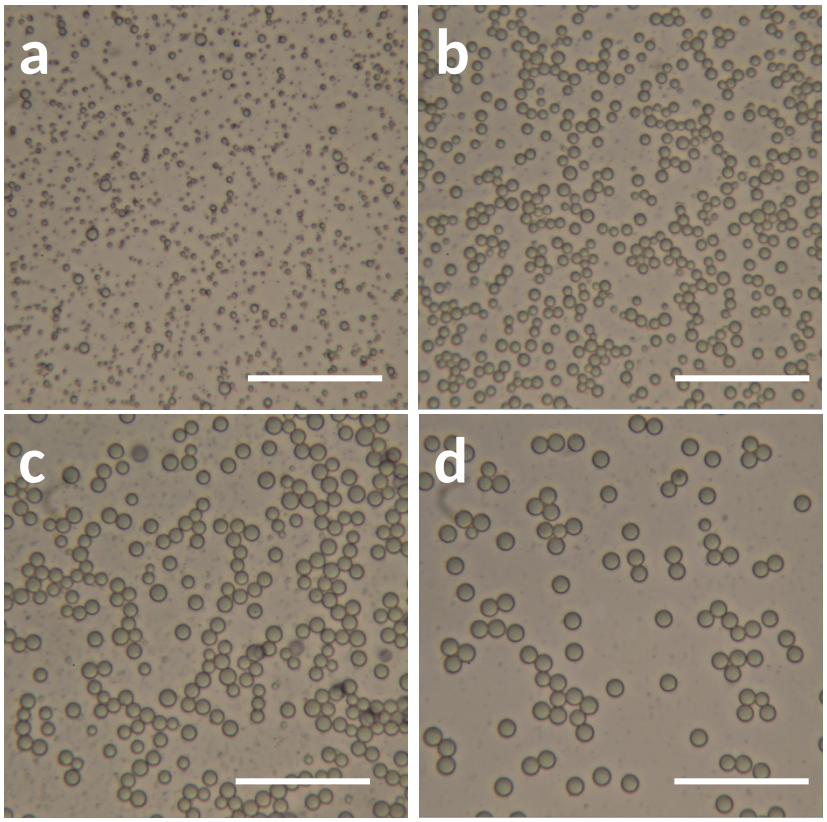

Fig. 3. Optical microscopy image of Pickering emulsions after 24 h for different volume ratio of water to oil phase (a) 10:1, (b) 10:2, (c) 10:3 and (d) 10:4. Length of unlabelled scale bar equals to 50 μm.

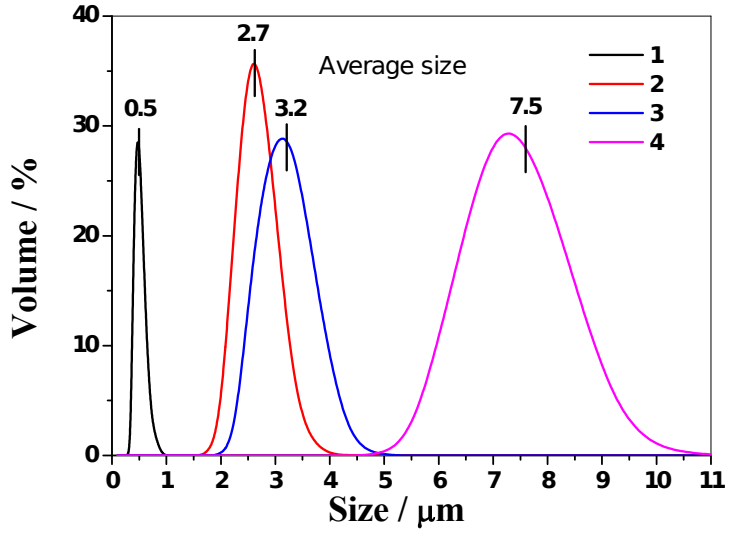

Fig. 4. Droplets size distributions for different volume ratio of water to oil phase measured by Dynamic Light Scattering: (1) 10:1, (2) 10:2, (3) 10:3 and (4) 10:4.

Optical microscopy images (Fig. 3) showed that the emulsion droplets were nicely dispersed in a continuous water phase. The average droplet size of emulsions underwent an evident change when the volume fraction of oil was varied. Additional water phases implied an increase in silica nanoparticle mass fraction. The Pickering emulsions were small when the number of particles used to stabilize the emulsion was large [21,31]. The dynamic light scattering of all emulsions was performed to provide detailed information about the size distribution of the droplets, as shown in Figure 4. The average sizes of the emulsions were 0.5, 2.7, 3.2, and 7.5 μm when the volume ratios of water to oil phase were 10:1, 10:2, 10:3, and 10:4, respectively.

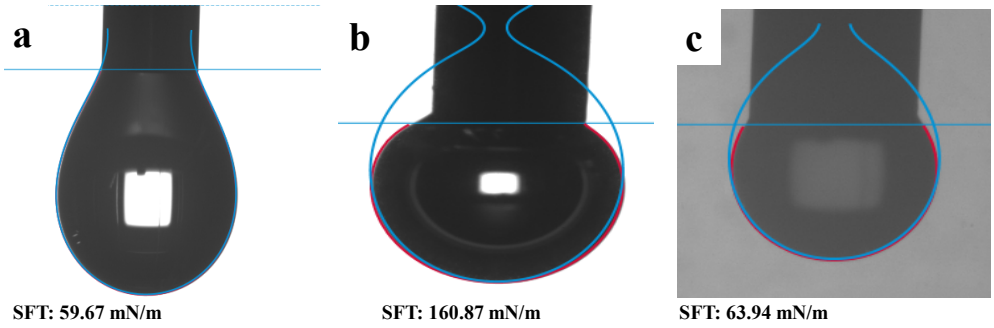

Fig. 5. Surface tension of linseed oil against air (a), water (b) and 3 wt% Ludox TMA suspension(c).

Additionally, surface tension of linseed oil against air, water, and Ludox TMA suspension was employed to confirm the stability of Pickering emulsion. In general, more hydrophilic particles can stabilize o/w emulsions and more hydrophobic particles can stabilize w/o emulsions. Grafted silica particles are often used for the stabilization of Pickering emulsions [32-34]. Justyna et al. [35] prepared a series of Pickering emulsions using fully hydrophilic silica nanoparticles and pointed out that the oil−water surface tension was a relevant criterion for oil selection. Figure 5 shows the surface tension of linseed oil against (a) air, (b) water and (c) 3 wt% Ludox TMA suspension. These pictures were taken at the instant when the biggest droplets were formed. The surface tension of linseed oil against air is 59.67 mN/m, which is lower than that of water (72.86 mN/m). Figures 5 (b) and (c) show that surface tension of linseed oil underwent a sharp decrease from 160.87 to 63.94 mN/m after 3 wt% Ludox TMA was added to the water. This reduction was attributed to the adsorbed solid particles at the oil/water interface, which provides emulsion stability.

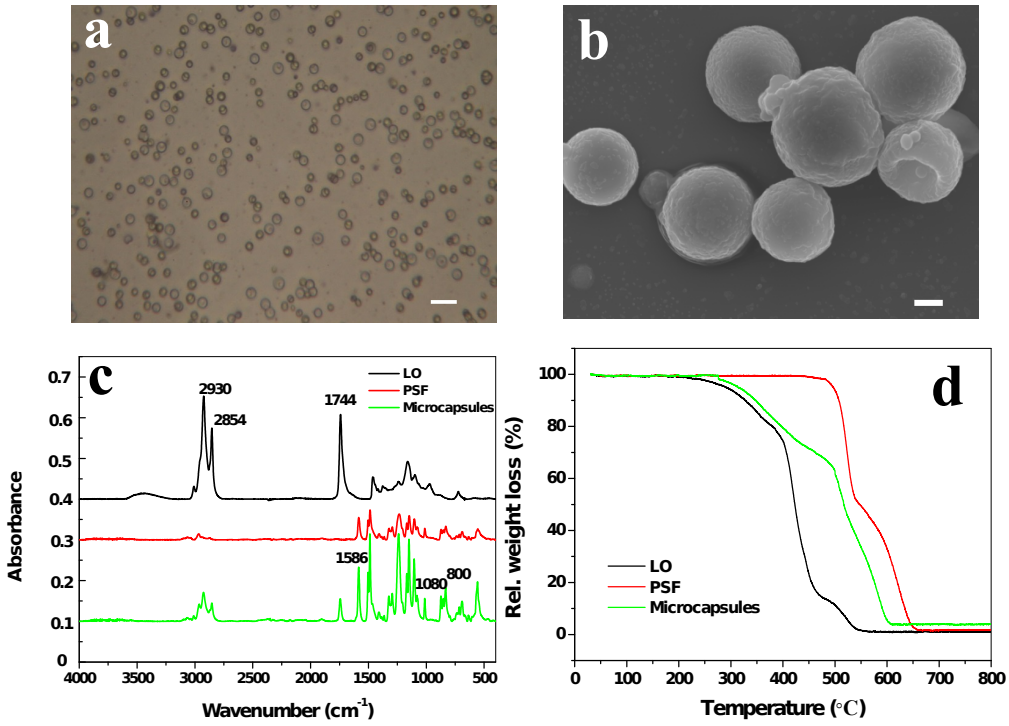

Fig. 6. (a) Optical microscopy image of microcapsules dispersed in cyclohexane (length of unlabelled scale bar equals 50 μm), (b) SEM image of microcapsules (length of unlabelled scale bar equals 1 μm), (c) ATR-FTIR spectra of linseed oil (LO), PSF, and microcapsules, (d) TGA curves for linseed oil (LO), PSF and unmodified microcapsules.

Many hydroxyl groups on the surface of microcapsules were identified before modification. These hydroxyl groups were dispersed well in water and suitable for waterborne coatings. These microcapsules aggregate together in water as most of the hydroxyl groups reacted with the QC18 after modification. Organic solvents were selected to disperse the modified microcapsules. Figure 6 (a) displays a homogeneous distribution of QC18-modified microcapsules in cyclohexane. Most of the particles maintained sufficient interparticle distances, indicating their potential application in solvent-borne coatings.

The SEM results of microcapsules are shown in Figure 6 (b). The microcapsules have a raspberry-like surface due to the silica aggregates in the shell. The image at higher magnification can be found in Figure S4 of Supporting Information section. No evidence of coalescence and collapsed structures was identified. A dimple-like structures were be found on the SEM image. This structures could be a result of the high energy beam of electrons and the vacuum condition under SEM observation. As a rough estimate, the diameter of microcapsules was approximately 4−6 μm.

To further assess the chemical structure of microcapsules, Fourier transform infrared spectroscopy and thermal gravimetric analysis of linseed oil, PSF, and modified microcapsules were carried out. The ATR-FTIR spectra of linseed oil, PSF, and modified microcapsules are presented in Figure 6 (c). The absorption peaks at 2930, 2854, 1744, and 1458 cm^{-1} correspond to =C−H stretching, C−H stretching, C=O stretching, and C−H bending, respectively. All these peaks are characteristic for linseed oil [36]. The spectrum of PSF shows characteristic peaks at 1489, 1504, 1586 cm^{-1} (C=C aromatic rings stretching), 1323, 1295 cm^{-1} (O=S=O asymmetric stretching), and 1230 cm^{-1} (C-O-C asymmetric stretching) [25]. The spectrum of filled microcapsules displays the characteristic peaks of linseed oil and the absorption band characteristics of the PSF. The absorption peaks at 800 and 1080 cm^{-1} correspond to Si−O−Si symmetric stretching and Si−O asymmetric vibration, respectively. All these peaks are characteristics of SiO_2. The ATR-FTIR results confirmed the successful encapsulation of linseed oil in microcapsules. Furthermore, no broad –OH peak at approximately 3400

cm^{-1} was identified because most of the hydroxyl groups reacted with QC18. The nanoparticles on the surface of the microcapsules have a Janus-like structure, as shown in Figure 1, with one side embedded inside the shell and the other side modified with QC18, which rendered the microcapsule antibacterial function.

The TGA curves of unmodified microcapsules, linseed oil, and PSF were obtained from 30 ºC to 800 ºC under N_2 protection to determine the loading capacity of microcapsules. As shown in Figure 6 (d), the decomposition of pristine linseed oil started at 300 ºC with a fast weight loss rate between 400 ºC and 450 ºC [37]. Decomposition stopped at 540 ºC without any residues. The PSF started to decompose at 500 ºC and finished at 650 ºC [25]. The TGA curve of unmodified microcapsules could be divided into two parts. The 40 wt% weight loss of microcapsules is mainly attributed to the calcination of linseed oil between 300 ºC to 500 ºC. The remaining mass was lost from 500 ºC to 600 ºC due to linseed and PSF decomposition. Results from the TGA analysis confirmed that at least 40 wt% of linseed oil was encapsulated in the microcapsules.

Localized electrochemical impedance spectroscopy (LEIS) were carried out to confirm the self-healing effect provided by the microcapsules. Compared with conventional electrochemical impedance spectroscopy (EIS), LEIS provides more detailed information about the corrosion inhibition effect and self-healing mechanisms in a localized manner [38-41]. The EIS convolutes the separate responses of the coating and defect together; however, this convolution is not relevant if the focus is on the local self-healing effect of the coating. LEIS, which commonly uses a five-electrode

configuration, is based on the ratio of the applied AC voltage to the local AC current density (i_{local}). i_{local} is calculated in accordance with the Ohm's law (1), where d is the distance between the two probes, and κ is the conductivity of the electrolyte.

$$i_{local} = \frac{\Delta V_{local}}{d} \kappa \quad (1)$$

The local admittance is calculated by equation (2), where the applied voltage ($\Delta V_{applied}$) is the potential difference between the reference electrode and the working electrode [42].

$$Y_{local} = \frac{i_{local}}{\Delta V_{applied}} \quad (2)$$

Figure 7 shows the admittance mapping of the scratched coatings; the mapping was obtained in 3.5 wt% NaCl solution at different times of immersion up to 24 h. A low frequency (10 Hz) was selected because it can exhibit the self-healing process of scratched coatings fast and effectively [43]. After 3 h, the defect was evident in Figure 7 (a) on the micrograph and reflected in the admittance map as a large increase around the scratched area. The defect remains active for 24 h. The intelligent coating behaves completely different. No remarkable increase in the admittance in the defect zone was observed during the entire test period. This effect is responsible for the reduction of the corrosion activity of the substrate due to the release of linseed oil. Linseed oil forms a solid film through chemical reaction with oxygen, which has been used as a healing agent for many years [37,44]. In order to verify the results of LEIS, the tested samples

were observed through optical microscopy after removing coatings (Figure S5). In the case of the steel coated with intelligent coating (Figure S5 (b)), small corrosion area proves their self-healing functionality and better barrier properties. This is in accordance with the LEIS test.

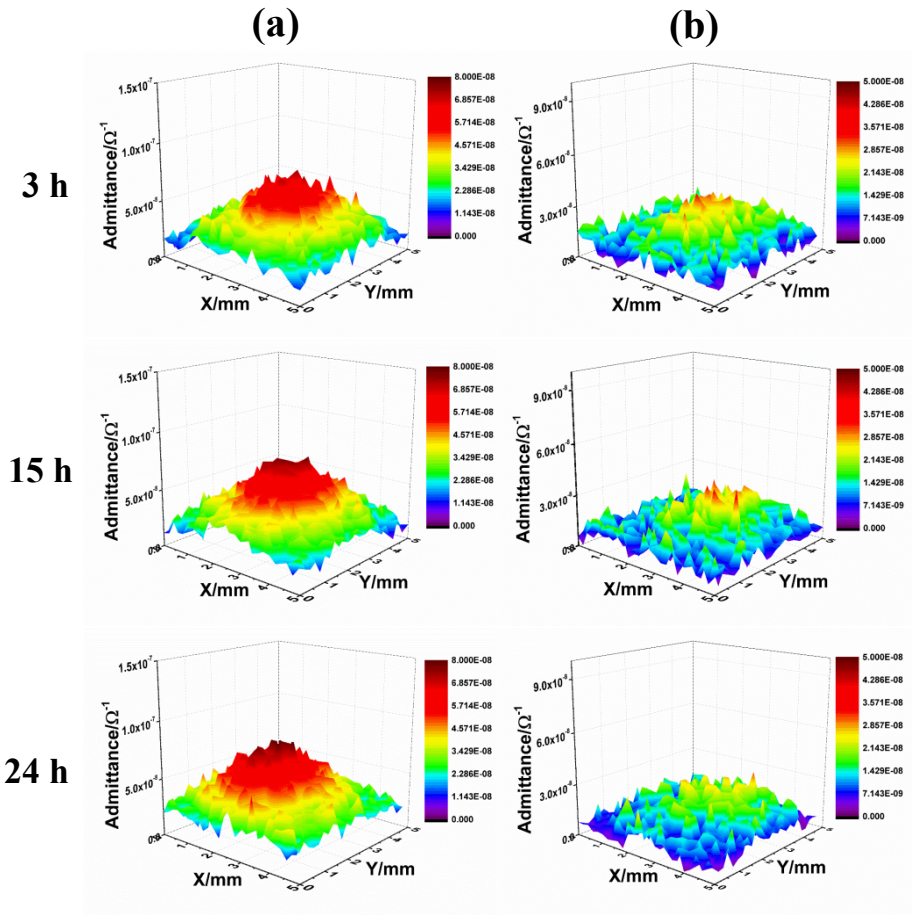

Fig. 7. Local admittance mappings performed at 10 Hz over the scratch after 3 h, 15 h and 24 h of immersion in 3.5 wt% NaCl for: (a) controlled coatings and (b) intelligent coating.

The second, antimicrobial effect of the microcapsules was demonstrated by the antibacterial experiments. The antibacterial efficacy of the QC18-modified capsules was evaluated against Gram-positive S. aureus and is presented in Figure 8(a). The photographs of the agar plates are given in Figure 8(b). The positive control sample was just the oil-encapsulated capsules without the presence of an active antimicrobial. All concentrations of the QC18-modofied capsules displayed antibacterial activity, which increased from QC18-oil0.5 sample showing an antimicrobial efficacy of 52% for the 5 and 10 mg/mL samples showing over 90% antimicrobial efficacy. Increasing the capsules' concentration further to 20 mg/mL decreased the antimicrobial efficacy to 86%. QC18 molecules tethered to the MSN particles killed the bacteria by interacting with the lipid bilayer structures of microbial cell membranes, thereby causing leakage and cell death.

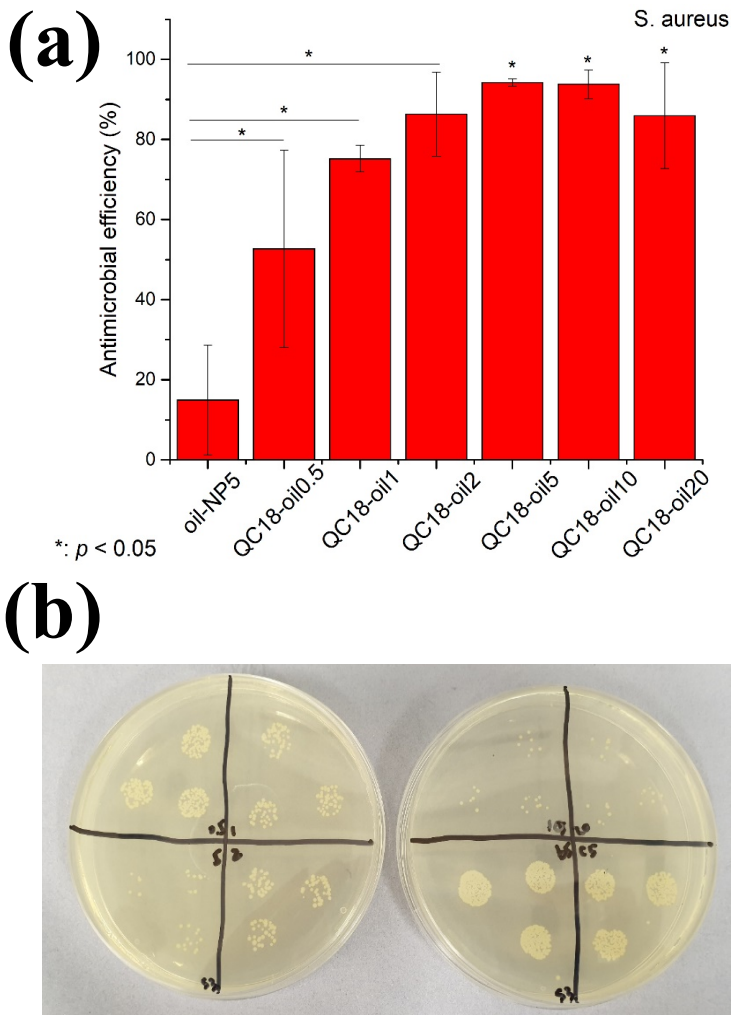

Fig. 8. (a) S.aureus inhibition efficiency of QC18 modified capsules (0.5, 1, 2, 5, 10, 20 mg/ml) and oil-encapsulated capsules (5mg/ml, as control group) after 3 h shaking incubation. (b) CFU agar plate read of QC18 modified capsules (0.5, 1, 2, 5, 10, 20 mg/ml) and oil-encapsulated capsules (5mg/ml, as control group) after 3 h shaking incubation. Presentative CFU image is the third run of the tests.

4. Conclusions

A novel type of microcapsule prepared via Pickering emulsion polymerization based on linseed oil-filled polysulfone/QC18-modified silica hybrid shell was reported. The chemical structure of microcapsules was confirmed via Fourier transform infrared spectroscopy and thermal gravimetric analysis. The microcapsules were embedded into an epoxy coating. The hybrid coating exhibited remarkable self-healing effect in the

scratched area filling it with polymer film formed by reaction of encapsulated linseed oil and atmospheric oxygen. A significant advantage compared to the other types of previously developed micro/nanocapsules is their outer surface modified by QC18, thus providing stable antimicrobial effect. This work paves a way for researchers to explore various multifunctional micro/nanocontainers, which can be obtained by choosing among various antimicrobial or anticorrosion agents. The ongoing research is focused on assessing the coatings under real seawater conditions to demonstrate the multifunctional micro/nanocontainers in actual industrial applications.

Declaration of Competing Interest

The authors declare no conflict of interest.

Acknowledgments

The authors are grateful for the financial support provided by Natural Science Foundation of China (51801110), Shandong Province Natural Science Foundation, China (ZR2017BD038, ZR2016DM21). The work was supported by ERC grant ENERCAPSULE (#647969). VV, PK and DS thank financial support from Russian Science Foundation (grant 19-79-30091) provided for antifouling and anticorrosion measurements.

References

[1] Y. Dong, Y. Lekbach, Z. Li, D. Xu, S. El Abed, S. Ibnsouda Koraichi, F. Wang, Microbiologically influenced corrosion of 304L stainless steel caused by an alga associated bacterium Halomonas titanicae, Journal of Materials Science & Technology 37 (2020) 200-206.

[2] Y. Li, C. Ning, Latest research progress of marine microbiological corrosion and bio-fouling, and new approaches of marine anti-corrosion and anti-fouling, Bioactive Materials 4 (2019) 189-195.
[3] G. Sun, H. Ge, J. Luo, R. Liu, Highly wear-resistant UV-curing antibacterial coatings via nanoparticle self-migration to the top surface, Prog. Org. Coat. 135 (2019) 19-26.
[4] W. Zhang, J.-X. Li, R.-C. Tang, A.-D. Zhai, Hydrophilic and antibacterial surface functionalization of polyamide fabric by coating with polylysine biomolecule, Prog. Org. Coat. 142 (2020) 105571.
[5] Y. Zhao, E. Zhou, D. Xu, Y. Yang, Y. Zhao, T. Zhang, T. Gu, K. Yang, F. Wang, Laboratory investigation of microbiologically influenced corrosion of 2205 duplex stainless steel by marine Pseudomonas aeruginosa biofilm using electrochemical noise, Corros. Sci. 143 (2018) 281-291.
[6] D.G. Shchukin, H. Möhwald, A Coat of Many Functions, Science 341 (2013) 1458-1459.
[7] K. S. Toohey, N. R. Sottos, J. A. Lewis, J. S. Moore, S. R. White, Self-healing materials with microvascular networks, Nat. Mater. 6 (2007) 581.
[8] S. R. White, N. R. Sottos, P. H. Geubelle, J. S. Moore, M. R. Kessler, S. R. Sriram, E. N. Brown, S. Viswanathan, Autonomic healing of polymer composites, Nature 409 (2001) 794-797.
[9] D. V. Andreeva, D. Fix, H. Möhwald, D. G. Shchukin, Self-Healing Anticorrosion Coatings Based on pH-Sensitive Polyelectrolyte/Inhibitor Sandwichlike Nanostructures, Adv. Mater. 20 (2008) 2789-2794.
[10] S. V. Lamaka, D. G. Shchukin, D. V. Andreeva, M. L. Zheludkevich, H. Möhwald, M. G. S. Ferreira, Sol-Gel/Polyelectrolyte Active Corrosion Protection System, Adv. Funct. Mater. 18 (2008) 3137-3147.
[11] D. G. Shchukin, H. Möhwald, Surface-Engineered Nanocontainers for Entrapment of Corrosion Inhibitors, Adv. Funct. Mater. 17 (2007) 1451-1458.
[12] D. G. Shchukin, M. Zheludkevich, K. Yasakau, S. Lamaka, M. G. S. Ferreira, H. Möhwald, Layer-by-Layer Assembled Nanocontainers for Self-Healing Corrosion Protection, Adv. Mater. 18 (2006) 1672-1678.
[13] M. L. Zheludkevich, D. G. Shchukin, K. A. Yasakau, H. Möhwald, M. G. S. Ferreira, Anticorrosion Coatings with Self-Healing Effect Based on Nanocontainers Impregnated with Corrosion Inhibitor, Chem. Mater. 19 (2007) 402-411.
[14] Z. Zheng, X. Huang, M. Schenderlein, D. Borisova, R. Cao, H. Möhwald, D. Shchukin, Self-Healing and Antifouling Multifunctional Coatings Based on pH and Sulfide Ion Sensitive Nanocontainers, Adv. Funct. Mater. 23 (2013) 3307-3314.
[15] E. Shchukina, D. G. Shchukin, Nanocontainer-Based Active Systems: From Self-Healing Coatings to Thermal Energy Storage, Langmuir (2019).
[16] E. Shchukina, H. Wang, D. G. Shchukin, Nanocontainer-based self-healing coatings: current progress and future perspectives, Chem. Commun. 55 (2019) 3859-3867.
[17] F. Zhang, P. Ju, M. Pan, D. Zhang, Y. Huang, G. Li, X. Li, Self-healing mechanisms in smart protective coatings: A review, Corros. Sci. 144 (2018) 74-88.
[18] B. Qian, Z. Song, L. Hao, W. Wang, D. Kong, Self-Healing Epoxy Coatings Based on Nanocontainers for Corrosion Protection of Mild Steel, J. Electrochem. Soc. 164 (2017) C54-C60.

[19] B. Qian, Z. Zheng, M. Michailids, N. Fleck, M. Bilton, Y. Song, G. Li, D. Shchukin, Mussel-Inspired Self-Healing Coatings Based on Polydopamine-Coated Nanocontainers for Corrosion Protection, ACS Appl. Mater. Interfaces 11 (2019) 10283-10291.
[20] S. U. Pickering, CXCVI.—Emulsions, J. Am. Chem. Soc. 91 (1907) 2001-2021.
[21] B. P. Binks, Particles as surfactants—similarities and differences, Curr. Opin. Colloid Interface Sci. 7 (2002) 21-41.
[22] B. P. Binks, S. O. Lumsdon, Stability of oil-in-water emulsions stabilised by silica particles, Phys. Chem. Chem. Phys. 1 (1999) 3007-3016.
[23] M. F. Haase, D. O. Grigoriev, H. Möhwald, D. G. Shchukin, Development of Nanoparticle Stabilized Polymer Nanocontainers with High Content of the Encapsulated Active Agent and Their Application in Water-Borne Anticorrosive Coatings, Adv. Mater. 24 (2012) 2429-2435.
[24] M. F. Haase, D. Grigoriev, H. Moehwald, B. Tiersch, D. G. Shchukin, Encapsulation of Amphoteric Substances in a pH-Sensitive Pickering Emulsion, J. Phys. Chem. C 114 (2010) 17304-17310.
[25] H. Li, S. Li, Z. Li, Y. Zhu, H. Wang, Polysulfone/SiO2 Hybrid Shell Microcapsules Synthesized by the Combination of Pickering Emulsification and the Solvent Evaporation Technique and Their Application in Self-Lubricating Composites, Langmuir 33 (2017) 14149-14155.
[26] M. Tischer, G. Pradel, K. Ohlsen, U. Holzgrabe, Quaternary Ammonium Salts and Their Antimicrobial Potential: Targets or Nonspecific Interactions?, Chemmedchem 7 (2012) 22-31.
[27] M. Michailidis, I. Sorzabal-Bellido, E. A. Adamidou, Y. A. Diaz-Fernandez, J. Aveyard, R. Wengier, D. Grigoriev, R. Raval, Y. Benayahu, R. A. D'Sa, D. Shchukin, Modified Mesoporous Silica Nanoparticles with a Dual Synergetic Antibacterial Effect, ACS Appl. Mater. Interfaces 9 (2017) 38364-38372.
[28] C. Liu, H. Zhao, P. Hou, B. Qian, X. Wang, C. Guo, L. Wang, Efficient Graphene/Cyclodextrin-Based Nanocontainer: Synthesis and Host–Guest Inclusion for Self-Healing Anticorrosion Application, ACS Appl. Mater. Interfaces 10 (2018) 36229-36239.
[29] A. A. Miles, S. S. Misra, J. O. Irwin, The estimation of the bactericidal power of the blood, Epidemiol. Infect. 38 (2009) 732-749.
[30] G. Fleming, J. Aveyard, J. L. Fothergill, F. McBride, R. Raval, R. A. D'Sa, Nitric Oxide Releasing Polymeric Coatings for the Prevention of Biofilm Formation, Polymers 9 (2017) 601.
[31] R. Aveyard, B. P. Binks, J. H. Clint, Emulsions stabilised solely by colloidal particles, Adv. Colloid Interface Sci. 100-102 (2003) 503-546.
[32] B. P. Binks, J. A. Rodrigues, Types of Phase Inversion of Silica Particle Stabilized Emulsions Containing Triglyceride Oil, Langmuir 19 (2003) 4905-4912.
[33] B. P. Binks, J. H. Clint, Solid Wettability from Surface Energy Components: Relevance to Pickering Emulsions, Langmuir 18 (2002) 1270-1273.
[34] A. Schoth, K. Landfester, R. Muñoz-Espí, Surfactant-Free Polyurethane Nanocapsules via Inverse Pickering Miniemulsion, Langmuir 31 (2015) 3784-3788.
[35] J. Frelichowska, M.-A. Bolzinger, Y. Chevalier, Pickering emulsions with bare silica, Colloids Surf., A 343 (2009) 70-74.

[36] D. A. Leal, I. C. Riegel-Vidotti, M. G. S. Ferreira, C. E. B. Marino, Smart coating based on double stimuli-responsive microcapsules containing linseed oil and benzotriazole for active corrosion protection, Corros. Sci. 130 (2018) 56-63.
[37] C. Suryanarayana, K. C. Rao, D. Kumar, Preparation and characterization of microcapsules containing linseed oil and its use in self-healing coatings, Prog. Org. Coat. 63 (2008) 72-78.
[38] F. Zou, D. Thierry, Localized electrochemical impedance spectroscopy for studying the degradation of organic coatings, Electrochim. Acta 42 (1997) 3293-3301.
[39] J.-B. Jorcin, H. Krawiec, N. Pébère, V. Vignal, Comparison of local electrochemical impedance measurements derived from bi-electrode and microcapillary techniques, Electrochim. Acta 54 (2009) 5775-5781.
[40] M. W. Wittmann, R. B. Leggat, S. R. Taylor, The Detection and Mapping of Defects in Organic Coatings Using Local Electrochemical Impedance Methods, J. Electrochem. Soc. 146 (1999) 4071-4075.
[41] J. V. Nardeli, D. V. Snihirova, C. S. Fugivara, M. F. Montemor, E. R. P. Pinto, Y. Messaddecq, A. V. Benedetti, Localised corrosion assessement of crambe-oil-based polyurethane coatings applied on the ASTM 1200 aluminum alloy, Corros. Sci. 111 (2016) 422-435.
[42] L. V. S. Philippe, G. W. Walter, S. B. Lyon, Investigating Localized Degradation of Organic Coatings: Comparison of Electrochemical Impedance Spectroscopy with Local Electrochemical Impedance Spectroscopy, J. Electrochem. Soc. 150 (2003) B111-B119.
[43] A. S. Nguyen, N. Pébère, A local electrochemical impedance study of the self-healing properties of waterborne coatings on 2024 aluminium alloy, Electrochim. Acta 222 (2016) 1806-1817.
[44] M. Lazzari, O. Chiantore, Drying and oxidative degradation of linseed oil, Polym. Degrad. Stab. 65 (1999) 303-313.

TOC Graphic